Available online at www.sciencedirect.com
SCIENCE DIRECT®
Journal of Organometallic Chemistry 689 (2004) 1835–1842
Journal of Organometallic Chemistry
www.elsevier.com/locate/jorganchem

Ethylene polymerization catalyzed by substituted pyrazole nickel complexes

Simphiwe M. Nelana [a], James Darkwa [a,*], Ilia A. Guzei [b], Selwyn F. Mapolie [a]

[a] Department of Chemistry, University of the Western Cape, Private Bag X17, Bellville 7535, South Africa
[b] Department of Chemistry, University of Wisconsin at Madison, Madison, WI 53706 USA

Received 17 December 2003; accepted 3 March 2004

Abstract

(Pyrazole)nickel dibromide complexes, $(3,5\text{-}Me_2pz)_2NiBr_2$ (**1**), $(3\text{-}Mepz)_4NiBr_2$ (**2**), $(pz)_4NiBr_2$ (**3**) and $(3,5\text{-}^tBu_2pz)_2NiBr_2$ (**4**), were prepared by the reaction of the appropriate pyrazole with $(DME)NiBr_2$. Solid-state structures of these complexes show a direct relation between the steric bulk of the pyrazole ligand and structure, with more bulky ligands forming four-coordinate complexes (**1** and **4**) whereas the less bulky ligands formed six-coordinate complexes (**2** and **3**). Activation of selected complexes (**1** and **3**) with methylaluminoxane (MAO) produced species that catalyzed the polymerization of ethylene to form high density polyethylene.

Keywords: Pyrazole; Nickel; Solid-state structures; Ethylene polymerization

1. Introduction

Polyolefins are the most widely produced plastics in the world and have numerous applications [1]. Over the last eight years there has been a renewed interest in the use of late transition metal complexes as catalysts for olefin polymerization [1–7]. This followed the discovery by Brookhart and Gibson that late transition metal complexes can function as single site catalysts. Late transition metal complexes are also less oxophilic, which make the co-polymerization of ethylene with polar monomers possible [2,8]. The most dominant late transition metal catalysts in olefin polymerization are those based on nickel and palladium complexes with α-diimine ligands [2] or iron and cobalt complexes with bis(pyridylimine) ligands [3,4]. The nitrogen containing ligands in these complexes can be easily modified to give polyethylenes with different microstructures and high molecular weights. Such modified ligands form metal complexes that have been reported by several workers[5–8], and indicates that these modified nitrogen ligand metal complexes are active catalysts for olefin polymerization.

We recently reported that substituted pyrazole palladium complexes are active catalysts for ethylene polymerization [9]. In addition we also subsequently reported another class of palladium complexes, in which benzenedicarbonyl and benzenetricarbonyl linkers bridge pyrazolyl units [10]. These palladium complexes, with benzenecarbonyl linkers, are even better ethylene polymerization catalysts than the substituted pyrazole palladium complexes. Both systems demonstrate that pyrazole and pyrazolyl late transition metal complexes can be good olefin polymerization catalysts. The incorporation of a carbonyl group into the ligand in the second type of complexes translates into an increase in the electrophilicity of the metal centre and hence increased catalyst activity of the complexes.

There are reports in the literature that nickel catalysts do not generally follow similar patterns as their palladium analogues in polymerizing olefins [6,7]. For example large substituents on pseudoaxial sites in nickel catalysts for olefin polymerization is known to block these sites and reduces chain transfer [2a,11]; whilst their palladium analogues behave differently. Of interest to us was whether without large substituents on the pyrazole

* Corresponding author. Tel.: 27219593053; fax: 27219593055.
E-mail address: jdarkwa@uwc.ac.za (J. Darkwa).

0022-328X/$ - see front matter © 2004 Elsevier B.V. All rights reserved.
doi:10.1016/j.jorganchem.2004.03.005

ring, nickel analogues of the palladium complexes we reported recently [9] would produce oligomers and/or branched polymers; since small substituents on nickel α-diimine complexes are reported to produce either olefin oligomers or branched polymers [6b,6c].

Another aspect of our investigation involved structural elucidation of pyrazole nickel complexes that we used as catalyst precursors for the polymerization of ethylene. Various reports on the structure of substituted pyrazole nickel complexes have appeared in the literature [12]. One of these reports [13] proposes from spectroscopic data that 3,5-dimethylpyrazole form octahedral complexes with nickel dihalides (**A**). It is clear from our solid-state structural studies that the structure proposed for 3,5-dimethylpyrazole nickel dihalide is incorrect. We found two types of substituted pyrazole nickel dihalide complexes depending on the substituents. Dimethyl- and ditertiarybutylpyrazole ligands form four-coordinate nickel dihalide complexes, whilst 3-methylpyrazole and pyrazole ligands form six-coordinate nickel dihalides. Some of these complexes were investigated for their catalytic activity in polymerizing ethylene and the effect of substituents on the pyrazoles on the type of polymers produced. The current report shows that linear high density polyethylene can be produced with nitrogen containing ligand complexes of nickel that have no bulky substituents. It also shows that in the solid-state 3,5-dimethylpyrazole-nickel(II) bromide is a four-coordinate complex.

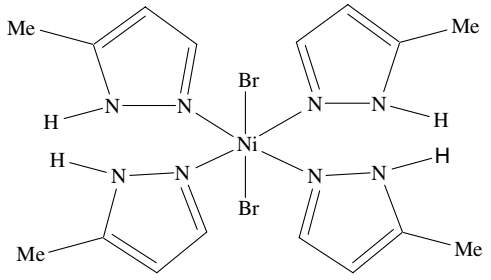

(X = Cl, Br)
A

2. Experimental

2.1. Materials and Instrumentation

All solvents were dried before use. Toluene and hexane were dried over sodium/benzophenone ketyl and dichloromethane was dried over phosphorus pentoxide. The starting materials 3,5-ditertbutylpyrazole [14] and (1,2-dimethoxyethane)nickel(II) bromide, [(DME)-$NiBr_2$], [15] were synthesized according to literature procedures. Other starting materials such as 3,5-dimethylpyrazole, 3-methylpyrazole and pyrazole were purchased from Sigma-Aldrich and used as received. All manipulations that are air and/or moisture-sensitive were performed under a dry, deoxygenated nitrogen atmosphere using standard high vacuum or Schlenk techniques. IR spectra were recorded as nujol mulls on a Perkin–Elmer, Paragon 1000 PC FT-IR spectrometer. NMR spectra were recorded on a Varian Gemini 2000 instrument (^1H at 200 MHz, ^{13}C at 50 MHz). Chemical shifts are reported in ppm and referenced to residual protons (7.26 ppm) and carbon signals (77.0 ppm) of $CHCl_3$ in $CDCl_3$. Elemental analysis was performed in-house on a Carlo Erba NA analyzer in the Department of Chemistry at the University of the Western Cape.

2.2. Synthesis of substituted pyrazole

2.2.1. $(3,5\text{-}Me_2pz)_2NiBr_2$ (**1**)

To an orange suspension of (DME)$NiBr_2$ (1.00 g, 3.25 mmol) in 20 ml CH_2Cl_2 was added 3,5-dimethylpyrazole (0.62 g, 6.50 mmol) in 20 ml CH_2Cl_2. The colour of the mixture immediately changed to dark blue. The mixture was stirred for 10 min, filtered and solvent removed to give a dark blue powder. Crystals suitable for X-ray analysis were obtained by slow diffusion of hexane into a CH_2Cl_2 solution of the compound, which was kept at −15 °C. Yield = 1.05 g (78%). Anal. Calc. for $C_{10}H_{16}Br_2N_4Ni$: C, 29.24; H, 3.93; N, 13.64. Found: C, 29.14; H, 3.86; N, 13.23%. IR (nujol mull, cm^{-1}): ν(N–H): 3225; ν(C=C): 1612; ν(C=N): 1564 (see Fig. 1).

2.2.2. $(5\text{-}Mepz)_4NiBr_2$ (**2**)

The preparation of **2** followed the same procedure as described for **1** in Section 2.2.1 starting with (DME)$NiBr_2$ (0.50 g, 1.62 mmol) and 3-methylpyrazole (0.27 g, 0.26 ml, 0.81 mmol). Light green crystals were obtained by slow evaporation of a CH_2Cl_2/hexane (1:1) solution of the product. Yield = 0.45 g (72%). Anal. Calc. for $C_{16}H_{24}Br_2N_8Ni$: C, 35.14; H, 4.42; N, 20.49. Found: C, 35.32; H, 4.21; N, 20.07%. IR (nujol mull, cm^{-1}): ν(N–H): 3291; ν(C=C): 1653; ν(C=N): 1561 (see Fig. 2).

2.2.3. $(pz)_4NiBr_2$ (**3**)

The preparation of **3** followed the same procedure as for **1** in Section 2.2.1 starting with (DME)$NiBr_2$ (1.00 g, 3.25 mmol) and pyrazole (0.44 g, 6.50 mmol). A pale blue powder was isolated and was found to be insoluble in most organic solvents. Yield = 0.80 g (69%). Anal. Calc. for $C_{12}H_{16}Br_2N_8Ni$: C, 29.37; H, 3.29; N, 22.83. Found: C, 28.98; H, 2.73; N, 21.92%. IR (nujol mull, cm^{-1}): ν(N–H): 3230; ν(C=C): 1622; ν(C=N): 1574.

2.2.4. $(3,5\text{-}^tBu_2pz)_2NiBr_2$ (**4**)

The preparation of **4** followed the same procedure as for **1** starting with (DME)$NiBr_2$ (0.90 g, 2.92 mmol) and

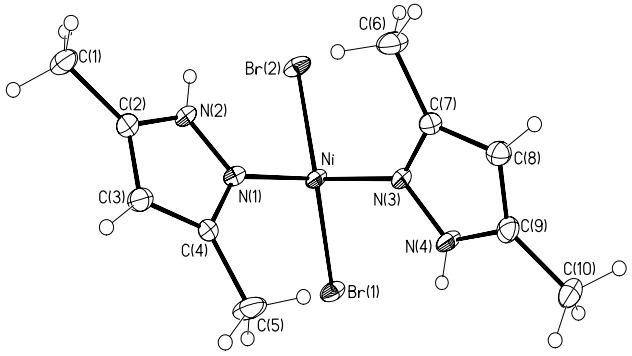

Fig. 1. ORTEP diagram of **1**. All atoms are drawn with 30% thermal probability ellipsoids.

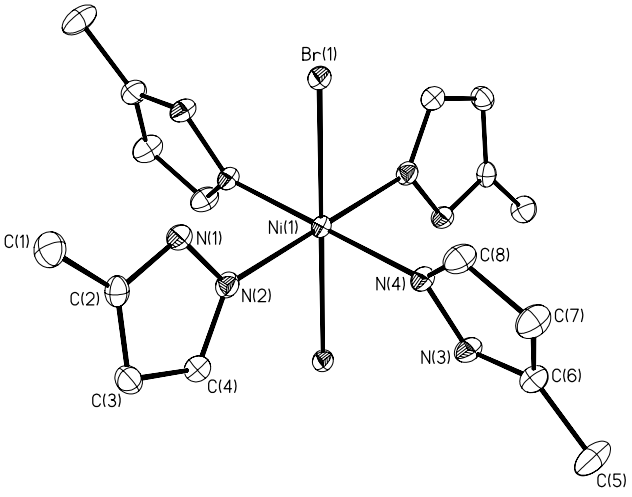

Fig. 2. ORTEP diagram of **2**. The labeled atoms comprise the asymmetric portion of the unit cell with Ni(1) located at the crystallographic inversion centre. All atoms are drawn with 50% thermal probability ellipsoids.

3,5-ditertbutylpyrazole (0.52 g, 5.84 mmol). A dark blue powder was isolated. Yield = 0.76 g (44%). Anal. Calc. for $C_{22}H_{40}Br_2N_4Ni$: C, 45.64; H, 6.96; N, 9.68. Found: C, 46.58; H, 8.32; 9.89%.

2.3. General procedure for ethylene polymerization

Polymerization was carried out in a 300 ml stainless steel autoclave, which was loaded with the catalyst and co-catalyst, methylaluminoxane (MAO), in a nitrogen purged glove box. This was done by charging the autoclave with a nickel complex in dry toluene (150 ml), and the appropriate amount of MAO (10% in toluene) at a co-catalyst to catalyst ratio ranging from 250 to 1000. The reactor was sealed and removed from the glove box and then flushed three times with ethylene after which it was heated to the polymerization temperature. Ethylene was continuously supplied to maintain a constant pressure during the polymerization reaction. After the set reaction time, excess ethylene was vented and the polymerization quenched by adding ethanol. The polymer was filtered, washed with 2 M HCl followed by ethanol and dried in an oven overnight at 50°C under vacuum.

NMR spectra of polyethylene were recorded in 1,2,4-trichlorobenzene/benzene-d^6 at 115 °C. The number-average (M_n) and weight-average (M_w) molecular weights and polydispersity (M_w/M_n) of the polymers were determined by high temperature gel permeation chromatography (GPC) (1,2,4-trichlorobenzene, 145 °C, rate = 1.000 ml/min) at the Group Technologies Research and Development laboratory of SASOL POLYMERS (South Africa) and the Institute of Polymer Science at the University of Stellenbosch (South Africa). Thermal analyses were performed on an Universal V2.3H TA instrument at the University of Botswana and on a Perkin–Elmer PC Series 7 system at the University of Cape Town (South Africa).

3. Results and discussion

3.1. Synthesis of substituted pyrazole nickel complexes

The complexes $(3,5\text{-}Me_2pz)_2NiBr_2$ (**1**), $(5\text{-}Mepz)_4NiBr_2$ (**2**), $(pz)_4NiBr_2$ (**3**) and $(3,5\text{-}^tBu_2pz)_2NiBr_2$ (**4**) were prepared in moderate to high yields according to Scheme 1. In the synthesis, $(DME)NiBr_2$ was suspended in dichloromethane and the appropriate pyrazole ligand in dichloromethane was added to this suspension. Complex **1** formed a dark blue solution immediately on addition of the ligand and the reaction was complete in 10 min. When the reaction was performed for longer periods, a pale blue dichloromethane insoluble material, which analysed as the dimeric complex **B** in Scheme 1, was isolated. Recently Laine et al. [6a] reported structures of a number of dimeric pyridinyliminenickel(II) complexes, featuring bridging bromo ligands, as proposed for **B**.

Similarly short reaction times for complex **2** gave soluble material, whilst long reaction times resulted in insoluble solids. However, preparation of **3** resulted in insoluble materials irrespective of reaction times. Various reports on the synthesis of complexes **1**–**3** have appeared in the literature [13,16–18] but none has related reaction times to the type of product isolated. We found reaction time to be crucial to the type of the product isolated. In particular complex **4** was highly unstable when kept in solution longer than 2 h, changing colour from bright blue to a dirty green solid. This is surprising since the palladium analogue is stable in solution indefinitely.

^{1}H NMR spectra of **1**, **2** and **4** had either broad peaks or none at all. This is typical of paramagnetic metal complexes and confirms that **1** and **4** have tetrahedral geometry. But for **2** to show paramagnetic behaviour, whilst its solid-state structure (vide infra) is octahedral,

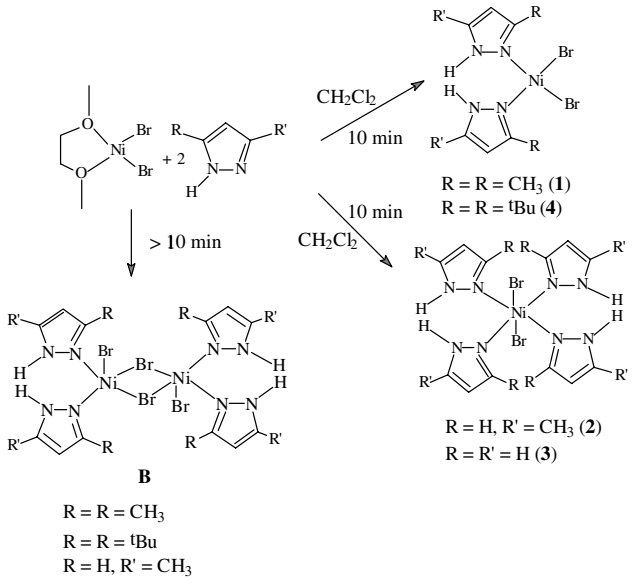

Scheme 1. Synthetic route to pyrazole nickel complexes.

suggest that in solution there is dissociation of pyrazole ligands to establish an equilibrium between diamagnetic octahedral species and paramagnetic tetrahedral species (Eq. 1). This equilibrium might also explain why **3** catalyses ethylene polymerization

$$(5\text{-Mepz})_4NiBr_2 \leftrightharpoons (5\text{-Mepz})_2NiBr_2 \quad (1)$$

3.2. Molecular structure of *1* and *2*

Solid-state structures of **1** and **2** were determined by X-ray crystallography (Table 1). The central Ni atom in complex **1** binds to two bromine atoms and two monodentate pyrazole ligands and exhibits a highly distorted tetrahedral geometry. The dihedral angle between the planes defined by atoms Ni, N(1), N(2) and Ni, Br(1), Br(2) measuring 79.61(8)° helps appreciate the distortion. The bond angles about the central metal vary between 98.90(12)° and 125.94(4)°. Steric repulsion between large bromine substituents results in a wide Br–Ni–Br angle of 125.94(4)° and causes the contraction of the N–Ni–N angle to 101.78(18)° (see Table 2).

The tetrahedral environment of the Ni atom in **1** is in contrast with the six-coordinate structure proposed by Poddar based on spectroscopic data [13]. It is difficult to see how **1** can exist as a six-coordinate compound, however Poddar does suggest that upon heating to 130–150 °C complex **1** converts to a four-coordinate tetrahedral complex. We have shown that this compound is tetrahedral in solid state at 293 and 173 K.

The Ni–Br distance in **1** (av. 2.373(9) Å) is in excellent agreement with the average Ni–Br distance of 2.36(3) Å in neutral tetrahedral nickel complexes. The latter value is obtained by averaging 72 bond distances in 45 relevant compounds reported to the Cambridge Structural Database (CSD) [19].

Complex **2** is six-coordinate with two bromine atoms in apical positions and four monodentate pyrazole ligands in the equatorial plane about a Ni centre. The geometry about the central metal is essentially undistorted octahedral with the *cis*-angles spanning between 88.87(7)° and 91.13(7)°. The Ni atom occupies a crystallographic inversion centre and only a half of the molecule is symmetry independent. The pyrazole ligands adopt a tautomeric form 5-methylpyrazole to facilitate

Table 1
Crystallographic data for complexes **1** and **2**

Parameter	**1**	**2**
Empirical formula	$C_{10}H_{16}Br_2N_4Ni$	$C_{16}H_{24}Br_2N_8Ni$
Formula weight	410.8	546.96
Temperature (K)	173(2)	100(2)
Wavelength (Å)	0.71073	0.71073
Crystal system	Monoclinic	Triclinic
Space group	$P2_1/n$	$P\bar{1}$
a (Å)	8.3441(11)	7.5408(4)
b (Å)	14.261(2)	8.5615(4)
c (Å)	12.4449(16)	3947(4)
α (°)	90	92.086(1)
β (°)	97.721	105.470(1)
γ (°)	90	114.453(1)
Volume (Å^3)	1467.5(3)	524.62(4)
Z	4	1
Density (calculated) Mg/m^3	1.859	1.731
Crystal size (mm^3)	$0.40 \times 0.30 \times 0.20$	$0.30 \times 0.30 \times 0.20$
Absorption correction	Empirical with SADABS	Empirical with SADABS
Max. and min. transmission	0.3453 and 0.1731	0.4500 and 0.3298
Final R indices [$I > 2\sigma(I)$]	$R1 = 0.0403$, $wR2 = 0.0938$	$R1 = 0.0244$, $wR2 = 0.0648$
Refinement method	Full-matrix least-squares on F^2	Full-matrix least-squares on F^2
R indices (all data) 0.1065	$R = 0.0787$, $wR2 = 0.1065$	$R1 = 0.0249$, $wR2 = 0.651$
Largest diff. peak and hole (e Å^{-3})	0.773 and −0.565	0.792 and −0.489

Table 2
Selected bond lengths [Å] and angles [°] for **1**

Bond lengths			
Ni–N(1)	1.971(4)	N(4)–C(9)	1.356(7)
Ni–N(3)	1.975(4)	C(1)–C(2)	1.505(6)
Ni–Br(1)	2.3791(8)	C(2)–C(3)	1.366(7)
Ni–Br(1)	2.3662(9)	C(3)–C(4)	1.384(7)
N(1)–N(2)	1.354(5)	C(4)–C(5)	1.484(7)
N(1)–C(4)	1.358(6)	C(6)–C(7)	1.495(7)
N(2)–C(2)	1.348(7)	C(7)–C(8)	1.390(7)
N(3)–C(7)	1.335(6)	C(8)–C(9)	1.360(7)
N(3)–N(4)	1.367(5)	C(9)–C(10)	1.492(7)
Bond angles			
N(1)–Ni–N(3)	101.78(18)	N(2)–C(2)–C(3)	105.6(5)
N(1)–Ni–Br(2)	98.90(12)	N(2)–C(2)–C(1)	121.8(5)
N(3)–Ni–Br(2)	113.45(12)	C(3)–C(2)–C(1)	132.6(5)
N(1)–Ni–Br(1)	115.14(12)	C(2)–C(3)–C(4)	107.9(5)
N(3)–Ni–Br(1)	99.73(12)	N(1)–C(4)–C(3)	109.0(4)
Br(2)–Ni–Br(1)	125.94(12)	N(1)–C(4)–C(5)	120.6(5)
N(2)–N(1)–C(4)	105.1(4)	C(3)–C(4)–C(5)	130.4(5)
N(2)–N(1)–N	122.9(3)	N(3)–C(7)–C(8)	109.5(5)
C(4)–N(1)–Ni	132.0(3)	N(3)–C(7)–C(6)	121.4(5)
C(2)–N(2)–N(1)	112.4(4)	C(8)–C(7)–C(6)	129.0(5)
C(7)–N(3)–N(4)	105.9(4)	C(9)–C(8)–C(7)	107.4(5)
C(7)–N(3)–Ni	132.1(3)	N(4)–C(9)–C(8)	106.3(5)
N(4)–N(3)–Ni	122.0(3)	N(4)–C(9)–C(10)	121.1(5)
C(9)–N(4)–N(3)	110.9(4)	C(8)–C(9)–C(10)	132.6(5)

Table 3
Selected bond lengths [Å] and angles [°] for **2**

Bond lengths			
Ni–Br(1)	2.6617(2)	N(3)–C(6)	1.345(3)
Ni–Br(1)#1	2.6617(2)	N(3)–N(4)	1.357(3)
Ni–N(2)	2.0996(18)	N(4)–C(8)	1.333(3)
Ni–N(2)#1	2.0996(18)	C(1)–C(2)	1.498(3)
Ni–N(4)	2.1004(18)	C(2)–C(3)	1.378(3)
Ni–N(4)#1	2.1004(18)	C(3)–C(4)	1.398(3)
N(1)–C(2)	1.343(3)	C(5)–C(6)	1.496(3)
N(1)–N(2)	1.360(3)	C(6)–C(7)	1.375(3)
N(2)–C(4)	1.335(3)	C(7)–C(8)	1.399(3)
Bond angles			
N(2)–Ni–N(2)	180.0	C(4)–N(2)–Ni	133.72(15)
N(2)–Ni–N(4)	88.87(7)	N(1)–N(2)–Ni	121.92(14)
N(2)#1–Ni–N(4)	91.13(7)	C(6)–N(3)–N(4)	112.70(19)
N(2)–Ni–N(4)#1	91.13(7)	C(8)–N(4)–N(3)	104.38(18)
N(2)#1–Ni–N(4)#1	88.87(7)	C(8)–N(4)–Ni	133.18(15)
N(4)–Ni–N(4)#1	180.0	N(3)–N(4)–Ni	122.39(14)
N(2)–Ni–Br(1)#1	89.79(5)	N(1)–C(2)–C(3)	106.12(19)
N(2)#1–Ni–Br(1)#1	90.21(5)	N(1)–C(2)–C(1)	121.1(2)
N(4)–Ni–Br(1)#1	89.81(5)	C(3)–C(2)–C(1)	132.7(2)
N(4)#1–Ni–Br(1)#1	90.19(5)	C(2)–C(3)–C(4)	105.6(2)
N(2)–Ni–Br(1)	90.21(5)	N(2)–C(4)–C(3)	111.2(2)
N(2)#1–Ni–Br(1)	89.79(5)	N(3)–C(6)–C(7)	106.24(19)
N(4)–Ni–Br(1)	90.19(5)	N(3)–C(6)–C(5)	122.0(2)
N(4)#1–Ni–Br(1)	89.81(5)	C(7)–C(6)–C(5)	131.7(2)
Br(1)#–Ni–Br(1)	180.0	C(6)–C(7)–C(8)	105.5(2)
C(2)–N(1)–N(2)	112.85(18)	N(4)–C(8)–C(7)	111.2(2)
C(4)–N(2)–N(1)	104.27(18)		

Symmetry transformations used to generate equivalent atoms. #1: $-x+2, -y, -z+1$.

coordination to the metal. This arrangement yields a less encumbered steric environment as compared to a hypothetical one obtained with 3-methylpyrazole.

The Ni–Br distance in **2** (2.6617(2) Å) (see Table 3) is significantly longer than that in **1** due to the presence of four extra electrons in the anti-bonding molecular orbitals. The ''typical'' Ni–Br bond distance calculated by averaging 28 distances in 14 relevant complexes reported to the CSD was found to be 2.57(6) Å. The Ni–Br distance in **2** is appreciably longer, however the difference is not statistically significant given the large standard deviation for the averaged CSD value. The Ni–Br distance in **2** is second longest in octahedral nickel complexes. The only longer bond of 2.762 Å was observed in (*N*,*N*′-bis(2-(benzylthio)ethyl)-1,5-diazacyclo-octane)dibromonickel(II) [20] (see Table 3).

3.3. Ethylene polymerization

Complexes **1** and **3** were activated with MAO and used as catalysts for ethylene polymerization. Complex **2** was not included in the polymerization experiments due to its completely different structure compared to complexes **1**, **3** and **4**. And because of its instability in solution, complex **4** was not used in ethylene polymerization studies, as it was difficult to determine the integrity of this complex in solution.

The polymerization results are summarized in Table 4. This data shows that complex **3** formed a catalyst with a higher activity compared to the catalyst formed by complex **1** at 25 °C. At this temperature the turn over number (TON) for **3** compared to **1** is more than doubled (entry 1, TON is 249.48 kg/mol Ni h compared to entry 2, TON is 481.23 kg/Ni h). This higher activity of **3** might be due to better accessibility of the substrate to the catalyst, which allows for fast coordination and insertion of ethylene into the metal-alkyl bond. Compared to the palladium analogue, $(pz)_2PdCl_2$, which has an activity of 1131.90 kg/mol Pd.h at 30 °C [9], the activity of catalyst **3** was lower (316.27 kg/mol Ni h) even at 40 °C. This difference in activity between palladium and nickel pyrazole catalysts may be due to the square planar geometry of the palladium pyrazole catalyst, which is more suitable for olefin coordination and subsequent insertion for chain growth than the tetrahedral environment found for the nickel complexes studied in this report. This suggests that a square planar geometry around the metal centre is vital for the catalyst to be active in olefin polymerization.

Other conditions of the polymerization reactions were also varied. Most of the variations in the conditions of polymerization were performed with catalyst **1**, the more soluble of the two catalysts studied. By lowering the Al:Ni ratio from 1000:1 to 500:1, while keeping a constant pressure and temperature (entry 3), confirmed that the best co-catalyst to catalyst ratio is

Table 4
Ethylene polymerization data

Entry	Catalyst	Temperature (°C)	Al:Ni	Pressure (atm)	Mass (g)	TON (kg/mol h)	T_m[a] (°C)	M_n ($\times 10^6$)	M_w[b] ($\times 10^6$)	M_w/M_n[c]
1	**1**	25	1000	5	5.11	249.48	136.76	0.59	1.44	2.43
2	**3**	25	1000	5	8.84	481.23	133.83	0.61	1.24	2.03
3	**3**	25	500	5	3.01	164.01	134.08	0.71	1.60	2.24
4	**1**	40	1000	5	6.87	336.98	135.92	1.07	1.62	1.51
5	**3**	40	1000	5	5.80	316.27	134.50	0.35	0.72	2.03
6	**1**	60	1000	5	16.66	811.63	135.42	0.36	0.74	2.07
7	**1**	70	1000	5	23.87	1170.32	131.54	0.16	0.39	2.46
8	**1**	25	1000	1	0.25	12.41	136.42	1.66	3.86	2.32
9	**1**	25	1000	2	1.58	76.92	136.51	1.56	4.02	2.57
10	**1**	25	1000	3	2.13	104.37	136.60	1.82	4.06	2.23
11	**1**	25	1000	4	3.31	161.74	136.01	1.54	3.89	2.51
12	**1**	25	1000	10	7.45	1095.29	132.25	0.41	1.27	3.08
13	**1**	25	1000	25	18.63	2741.12	131.97	0.31	0.65	1.92
14	**1**	25	1000	30	23.39	3441.17	130.50	0.41	0.84	2.04

Reaction conditions: $[Ni] = 4.5 \times 10^{-5}$ M, toluene = 150 ml, polymerization time = 3 h.
[a] Melting point determined by DSC.
[b] Determined by GPC.
[c] Polydispersity by GPC.

1000:1. The polymers produced were characterized by gel permeation chromatography (GPC) to obtain their molecule weights and molecular weight distributions. The molecular weights of the polymers produced using **3** were lower than those produced by **1**. Molecular weights range between 0.72×10^6 and 1.6×10^6 g/mol for **3** compared to the molecular weight of about 4.01×10^6 g/mol for **1**. The molecular weights (M_w) of the polyethylene produced by catalyst **1** decrease with increasing temperature. The M_w decreases from 1.44×10^6 g/mol at 25 °C (entry 1) to 0.39×10^6 g/mol at 70 °C (entry 8). As temperature was increased catalyst activity increased, whilst polymer molecular weight decreased.

For most nickel olefin oligomerization or polymerization catalysts, increase in temperature generally results in catalyst deactivation. Such nickel catalysts deactivate at about 55 °C. There are, however, a few examples where nickel catalyst activity increases with increased temperature. For example two α-diimine nickel catalysts prepared from Ph–N=C(An)–C(An)=N–Ph and 4-MeC_6H_4–N=C(Me)–C(Me)=N–C_6H_4Me-4 show increased activity up to 75 °C without deactivation [6b]. Even catalysts that deactivate at high temperatures initially show increased turnovers before deactivation sets in at higher temperatures [6c,6d]. Catalysts **1** and **3** represent some of the rare examples of increase in nickel catalysts activity up to 70 °C, without deactivation of the catalysts. Increase in temperature normally produces lower molecular weight polymers. Comparing polymer molecular weights from the two catalysts, catalyst **1** gave polymers with higher molecular weights than those from catalyst **3** (Table 4). The trend of polymer molecular weight, however, appears not to be dependent on steric factors as the less sterically hindered **3** generally produced lower molecular weight polymers.

Molecular weights of polymers were also affected by pressure. Increasing the pressure of the monomer had two effects. First, increase in pressure resulted in increased activity of catalysts (Fig. 3). As pressure increase gives higher monomer concentration, insertion of monomer should be more rapid at higher concentrations. Secondly, increase in pressure gave lower polymer molecular weights. Fig. 4 shows the dependence of molecular weight on pressure. But generally polymer molecular weight distribution, measured by polydispersity indices, showed that they were approximately 2 and similar to distribution reported for other late-transition metal catalyzed ethylene polymerization [2–10].

NMR spectroscopy was used to determine the microstructures of the polyethylene produced. High tem-

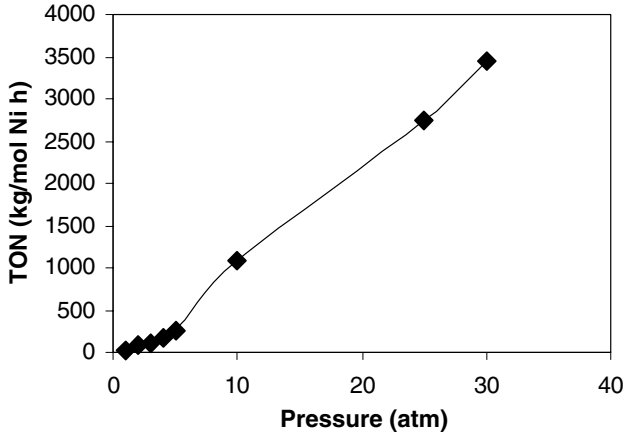

Fig. 3. Effect of pressure on catalyst activity.

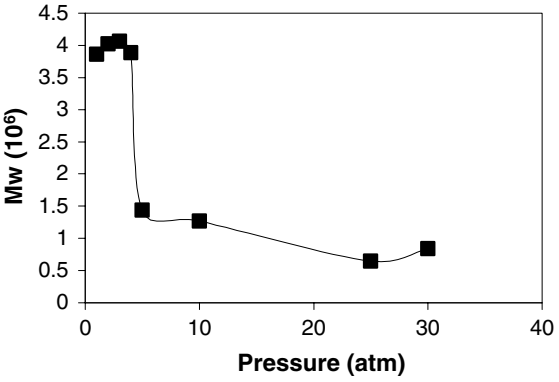

Fig. 4. Effect of pressure on polyethylene molecular weight.

perature ^{1}H NMR and ^{13}C NMR spectra had single peaks at 1.47 and 30.2 ppm, respectively, for the polymers produced at both low and high pressures. This is typical of high-density polyethylene (HDPE). Further evidence of HDPE formation is provided by DSC data in Table 4. Melting points from the DSC measurements were found to be between 131 and 136 °C. There was not much change in polyethylene melting point with change in reaction conditions. At both low temperatures (25 and 40 °C, $T_m = 136.76$ and 135.95 °C) and high temperatures (60 and 70 °C, $T_m = 135.42$ and 131.54 °C), only a small decrease in melting point was observed. This trend is similar to melting point differences found when pressure is increased.

The formation of linear polyethylene indicates that there is no ''chain walking'' during polymerization reactions. Brookhart and co-workers have shown that, without bulky substituents in axial position, nickel-based catalysts produce oligomers via agostic interaction of the β-hydrogen atom with the metal centre. The use of bulky of substituents prevents agostic interactions and hence ''chain walking''. It is interesting to note that catalysts **1** and **3** without bulky substituents produce HDPE. For **1** and **3** to produce HDPE, monomer insertion has to be more rapid than agostic interactions in order to prevent ''chain walking''. Since pyrazoles are weaker σ-donors than α-diimines and pyridines, two ligands that form oligomerization catalysts, production of HDPE by **1** and **3** suggests catalysts **1** and **3** are more electrophilic than nickel α-diimines and pyridines catalysts. We believe the higher electrophilicity of **1** and **3** facilitates very rapid insertion of monomer and rapid chain growth, such that agostic interactions that lead to oligomers is much slower than monomer insertion. This would explain why **1** and **3** produce polymers rather than oligomers.

In summary, we have prepared pyrazole nickel complexes that have solid-state structures determined by substituents on the pyrazoles. Bulky pyrazoles form four-coordinate nickel complexes, whereas less bulky pyrazoles form six-coordinate complexes. Two of the nickel complexes, **1** and **3**, can be activated by MAO to form active catalysts for ethylene polymerization; although the activities of **1** and **3** are lower than the very active α-diimine nickel catalysts discovered by Brookhart. Our nickel catalysts are also less active than the palladium analogues recently reported by us [9]. The formation of linear polyethylene by **1** and **3**, which have no bulky axial substituents, is significant and could be the result of very rapid monomer insertion due to highly electrophilic catalytic centres in **1** and **3** that prevents ''chain walking''.

4. Supplementary material

Crystallographic data for structural analysis have been deposited with the Cambridge Crystallographic Data Centre, CCDC Nos 226860 and 226861. Copies of this information may be obtained free of charge from The Director, CCDC, 12 Union Road, Cambridge, CB2 1EZ, UK (fax: +44-1223-336063; e-mail: deposit@ccdc.cam.ac.ukor http://www.ccdc.cam.ac.uk).

Acknowledgements

Financial support by the National Research Foundation (NRF), South Africa (SMN, JD, SFM) is gratefully acknowledged. Also we thank Stefan de Goede, SASOL POLYMERS (South Africa), for assistance with GPC determination.

References

[1] I.L. Levowitz, Morden Plastics Encyclopedia '99, McGraw-Hill, New York, 75, 1999, pp. B3–B6.
[2] (a) L.K. Johnson, C.M. Killian, M. Brookhart, J. Am. Chem. Soc. 117 (1995) 6414;
(b) S.D. Ittel, L.K. Johnson, M. Brookhart, Chem. Rev. 100 (2000) 1169;
(c) D.P. Gates, S.A. Svejda, E. Oñate, C.M. Killian, L.K. Johnson, P.S. White, M. Brookhart, Macromolecules 33 (2000) 2320.
[3] (a) V.C. Gibson, P.J. Maddox, C. Newton, C. Redshaw, G.A. Solan, A.J.P. White, D.J. Williams, J. Chem. Soc., Chem. Commun. (1998) 1651;
(b) V.C. Gibson, C. Newton, C. Redshaw, G.A. Solan, A.J.P. White, D.J. Williams, J. Chem. Soc., Dalton Trans. (1999) 827.
[4] B.L. Small, M. Brookhart, Macromolecules 32 (1999) 2120.
[5] R.J. Maldanis, J.S. Wood, A. Chandrasekaran, M.D. Rausch, J.C.W. Chien, J. Organomet. Chem. 645 (2002) 158.
[6] (a) T.V. Laine, U. Piironen, K. Lappalainen, M. Klinga, E. Aitola, M. Leskela, J. Organomet. Chem. 606 (2000) 112;
(b) C.M. Killian, L.K. Johnson, M. Brookhart, Organometallics 16 (1997) 2005;
(c) S.A. Svejda, M. Brookhart, Organometallics 18 (1999) 65;
(d) T.V. Laine, U. Piironen, K. Lappalainen, J. Liimatta, E. Aitola, B. Lofgren, M. Leskela, Macromol. Rapid Commun. 20 (1999) 487.

[7] A. Koppl, H.G. Alt, J. Mol. Catal. A: Chem. 154 (2000) 45.
[8] E.F. Connor, T.R. Younkin, J.I. Henderson, S. Hwang, R.H. Grubbs, W.P. Roberts, J.J. Litzau Sci, J. Polym. Part A: Polym. Chem. 40 (2002) 2842.
[9] K. Li, J. Darkwa, I.A. Guzei, S.F. Mapolie, J. Organomet. Chem. 660 (2002) 108.
[10] I.A. Guzei, K. Li, G.A. Bikzhanova, J. Darkwa, S.F. Mapolie, Dalton Trans. (2003) 715.
[11] (a) L.K. Johnson, S. Mecking, M. Brookhart, J. Am. Chem. Soc. 118 (1996) 11664;
(b) L. Deng, T.K. Woo, L. Cavallo, P.M. Margl, T. Ziegler, J. Am. Chem. Soc. 119 (1997) 6177;
(c) S.A. Svejda, L.K. Johnson, M. Brookhart, J. Am. Chem. Soc. 121 (1999) 10634.
[12] S. Trofimenko, Chem. Rev. 72 (1972) 497.
[13] S.N. Poddar, Sci. Cult. 35 (1969) 28.
[14] J. Elguero, E.G.R. Jacquier, Bull. Soc. Chim. Fr. 2 (1968) 707.
[15] L.G.L. Ward, Inorg. Synth. 13 (1972) 154.
[16] C.W. Reimann, A. Santoro, A.D. Mighell, Acta Crystallogr. B 26 (1969) 595.
[17] C.W. Reimann, A.D. Mighell, F.A. Mauer, Acta Crystallogr. 23 (1967) 135.
[18] (a) J. Reedijk, Recl. Trav. Chim. Pays-Bas. 88 (1969) 1451;
(b) J. Reedijk, Recl. Trav. Chim. Pays-Bas. 89 (1970) 605.
[19] F.H. Allen, Acta Crystallogr. B 58 (2002) 380.
[20] R.M. Buonomo, J.H. Reibenspies, M.Y. Darensbourgh, Chem. Ber. 129 (1999) 779.